

Navier-Stokes Methods to Predict Circulation Control Airfoil Performance

S. L. Williams*

Aeronautical Systems Division, Wright-Patterson Air Force Base, Ohio 45433
and

M. E. Franke†

Air Force Institute of Technology, Wright-Patterson Air Force Base, Ohio 45433

The predictive capability of the two-dimensional, compressible, mass-averaged, Navier-Stokes equations is investigated for a typical circulation control airfoil. The governing equations are solved using the implicit approximate-factorization algorithm of Beam-Warming with the turbulence model of Baldwin-Lomax. To account for the unique characteristics of circulation control airfoils, an empirical turbulence model correction for curved shear-layer flows is employed. The predictive capability of the computational method is explored by examining the importance of the curvature correction constant on the computed results.

Nomenclature

| | |
|----------------|--|
| C_d | = section drag coefficient |
| C_l | = section lift coefficient |
| $C_{m.s}$ | = section midchord moment coefficient |
| C_p | = pressure coefficient |
| C_μ | = blowing momentum coefficient |
| c | = airfoil chord |
| F | = curvature correction factor |
| h | = jet-slot height |
| l | = turbulence model mixing length |
| M_∞ | = freestream Mach number |
| \dot{m} | = jet mass flow rate |
| n | = local normal coordinate direction |
| P | = static pressure |
| P_t | = jet total pressure |
| q_∞ | = freestream dynamic pressure |
| Re | = Reynolds number |
| r | = local streamline radius of curvature |
| S | = turbulence model curvature term |
| T | = static temperature |
| T_t | = jet total temperature |
| U | = local velocity |
| U_∞ | = freestream velocity |
| u, v | = cartesian velocity components |
| V | = jet velocity |
| x, y | = cartesian coordinates |
| α | = airfoil angle of attack |
| α_{eff} | = airfoil effective angle of attack |
| β | = jet detachment angle |
| θ | = curvature constant |
| μ | = viscosity |
| μ_t | = turbulent eddy viscosity |
| ρ | = static density |
| ω | = vorticity |

Subscripts

NS = Navier-Stokes

wt = wind tunnel
 ∞ = freestream conditions

Introduction

THE development of vertical or short takeoff and landing (V/STOL) aircraft with conventional aircraft cruise performance has long been a goal of aircraft design engineers. Kohlman¹ describes requirements and advantages that should be considered in the development and implementation of V/STOL type aircraft. For example, V/STOL aircraft with steeper climbout and approach paths would reduce airport land requirements and would expose a smaller land area to noise. V/STOL aircraft with decreased landing speeds may also improve safety. For the military, the use of V/STOL aircraft would lessen the dependence on undamaged runways for operational capability.

Unfortunately, designing a V/STOL aircraft with conventional aircraft performance is not an easy task. To gain V/STOL performance, devices must be added to an aircraft that degrade its cruise performance either through external changes to the aircraft or additional weight. For STOL aircraft, many different concepts have been proposed over the years. One such promising concept is circulation control.^{2–4}

Circulation control airfoils and wings make use of the Coanda effect (flow attachment to a surface) by blowing a small, high-velocity jet over a rounded airfoil trailing edge. Since the airfoil trailing edge is not sharp, as on conventional airfoils, the Kutta condition is not fixed, but set by the amount of airfoil blowing. With blowing, the front and rear stagnation points move toward the lower airfoil surface to provide increased circulation and, hence, increased lift.

Use of this concept offers certain advantages over conventional airfoils such as much higher lift coefficients. This allows an aircraft to take off and land at greatly reduced speeds with the same value of lift. There are also disadvantages in that circulation control airfoils with their rounded trailing edges have poorer performance at cruise speeds when compared with conventional airfoils, although certain designs can accommodate cruise requirements.² The use of blowing also requires the addition of pressurized ducts to the aircraft resulting in increased aircraft weight.

Circulation Control Numerical Methods

Determining the performance of circulation control airfoils using theoretical or computational methods has proven to be extremely difficult due to the complex flowfield involved. The

Presented as Paper 90-0574 at the AIAA 28th Aerospace Sciences Meeting, Reno, NV, Jan. 8–11, 1990; received April 23, 1990; revision received Feb. 20, 1991; accepted for publication April 16, 1991. This paper is declared a work of the U.S. Government and is not subject to copyright protection in the United States.

*Aerospace Design Engineer, Development Planning. Member AIAA.

†Professor. Associate Fellow AIAA.

flow over a circulation control airfoil is greatly complicated by the rounded trailing edge, or Coanda surface, and the introduction of jet blowing. The jet boundary-layer detachment from the Coanda surface must be accurately found due to the great sensitivity of lift to the forward and aft stagnation point locations. The wall-jet flow from the slot also introduces a second boundary layer into the flowfield with different length scales than the conventional airfoil boundary layer. In addition, a free shear layer is formed between the oncoming airfoil upper-surface boundary layer and the wall-jet flow. Also, as the jet blowing increases, so does the influence of compressibility, even at relatively low freestream Mach numbers.

Due to the highly-coupled, nonlinear behavior of the flowfield, the Navier-Stokes equations appear to offer the best hope of solving this complicated problem. Solutions using coupled lesser approximations of the Navier-Stokes equations do not appear to offer the needed accuracy for circulation control airfoil design purposes.^{3,4} However, even Navier-Stokes methods are challenged due to the lack of accurate turbulence models for highly curved flows with strong adverse pressure gradients.^{3,5}

Several studies using Navier-Stokes methods to evaluate circulation control airfoil performance have been conducted.⁵⁻⁹ Berman⁹ solved for the flow over a circulation control airfoil using TRACON over the first 50% of the airfoil chord and a MacCormack explicit solver with the Baldwin-Lomax turbulence model over the aft 50% chord. This method was able to obtain solutions showing correct trends with the experimental pressure coefficient distribution; however, the magnitudes of the computed pressure coefficients were not as large as those found experimentally.

Shrewsbury⁶⁻⁸ examined the use of an implicit formulation of the compressible Reynolds-averaged, Navier-Stokes equations with a modified form of the Baldwin-Lomax turbulence model.¹⁰ Jet-slot boundary conditions were set at the slot exit, and a correction given by Bradshaw¹¹ was applied to the turbulence model to account for the curvature of the Coanda surface. Several airfoils at different flight conditions were examined. This method performed well and provided lift and pressure coefficient results in close agreement with experimental data. Although good overall agreement was reached, Shrewsbury⁶ concluded that better turbulence models were needed to resolve the jet detachment from the Coanda surface.

Pulliam et al.⁵ also employed an implicit formulation of the Navier-Stokes equations with the Baldwin-Lomax turbulence model to compute the flow over circulation control airfoils. Pulliam et al. used a spiral grid that extended from the jet plenum chamber through the slot exit and was wrapped about the airfoil. Use of this unique grid scheme allowed the flow to be computed rather than modeled at the jet-slot exit. This study examined two different circulation control airfoils at various flight conditions and obtained results in close agreement with experiment. However, since the results were not completely predictive, due to the need to adjust the turbulence model for different cases, Pulliam et al. also concluded that better turbulence models were needed.

These papers⁵⁻⁹ have demonstrated that the Navier-Stokes equations can indeed provide good estimates of the lift and pitching moment of circulation control airfoils at various flight conditions provided the turbulence model is able to give a reasonably good estimate of the jet separation point from the Coanda surface. The turbulence model curvature corrections used by both Shrewsbury⁶⁻⁸ and Pulliam et al.⁵ contain an empirical constant term whose magnitude is dependent on the type of airfoil Coanda surface and the freestream Mach number of the flow. Thus, to obtain solutions of comparable accuracy, one must, through trial and error, determine the value of the empirical constant that yields a computational solution in close agreement with the experimental data.

The purpose of this study is to explore further the predictive capability of Navier-Stokes methods in determining the lift,

drag, and moment performance of circulation control airfoils. To accomplish this goal, a computational method similar to the one used by Shrewsbury⁶ is developed and applied to a typical circulation control airfoil. The method used in this study solves the two-dimensional, compressible, mass-averaged, Navier-Stokes equations using the implicit approximate-factorization algorithm of Beam-Warming.¹² Closure of these equations for turbulent flows is obtained using the Baldwin-Lomax¹⁰ turbulence model with a curvature correction described by Bradshaw.¹¹ This study examines the importance of the empirical turbulence model correction in obtaining accurate predictions of airfoil performance at various values of the blowing momentum coefficient. This is done by applying the method with a predefined value of the empirical curvature constant and then comparing the results with experiment. Finally, the sensitivity of the computational results to a range of values of the curvature constant is explored.

Numerical Approach

The Navier-Stokes solver chosen for use in this study is described by Visbal,^{13,14} Visbal and Shang,¹⁵ and Steger.¹⁶ Modifications to this method consisted of modifying the airfoil boundary conditions to account for jet-slot blowing and employing the turbulence model curvature correction of Bradshaw¹¹ to account for the curvature of the Coanda surface. Details are given by Williams.¹⁷

Governing Equations

The governing equations are the two-dimensional, compressible, mass-averaged continuity, momentum, and energy equations. These equations, cast in strong-conservation form, are well documented in the literature¹³⁻¹⁶ and will not be repeated here. The perfect gas law, Sutherland's viscosity formula, a constant Prandtl number, and a modified version of the Baldwin-Lomax turbulence model are used with the governing equations.

The governing equations are solved numerically using the implicit approximate-factorization scheme of Beam-Warming.¹² In this formulation, first-order Euler time differencing is used while the spatial derivative terms are discretized using second-order-accurate central differences. Both explicit and implicit smoothing terms have been added to the algorithm for numerical stability and to capture embedded shocks.¹³ A variable time step can be employed for faster convergence to a steady-state solution. This solver is fully vectorized for use on parallel processing computers.

Boundary Conditions

The extent of the computational grid and the locations where boundary conditions are specified are illustrated in Fig. 1. Conventional airfoil boundary conditions are applied everywhere except at the jet-slot exit. At the inflow portion of the exterior grid, the velocity components, density, and pressure are specified at freestream conditions. At the outflow portion of the exterior grid, the pressure is set equal to the freestream static pressure with the gradient in the x direction of the other flow quantities, such as ρ , u , and v , set to zero. Along the grid cutline, a periodic boundary condition is enforced. On the airfoil surface, adiabatic, impermeable wall, and no-slip boundary conditions are applied.

Certain assumptions, based upon the work of Shrewsbury,⁶ are made to set the boundary conditions at the jet-slot exit. First, it is assumed that the jet total pressure and temperature are constant across the slot exit. Second, it is assumed that the isentropic relations provide a good approximation of the internal flow before the slot exit. Third, the jet nozzle is assumed to be convergent. With these assumptions, the jet-slot boundary conditions can be uniquely specified by extrapolating the latest solution static pressure distribution to the slot exit.

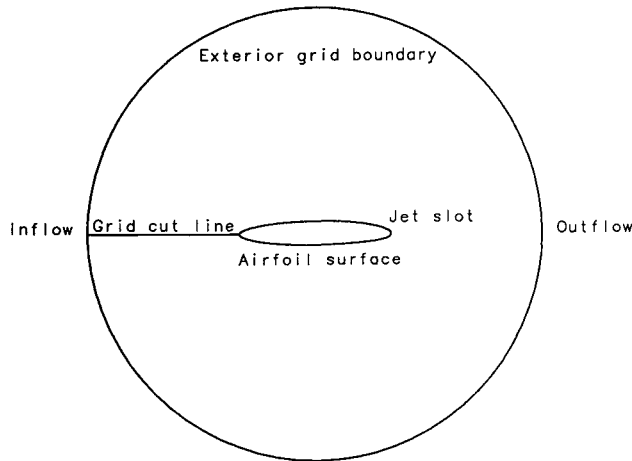


Fig. 1 Computational grid boundaries.

A jet momentum blowing coefficient is defined as

$$C_\mu = \frac{\dot{m}V}{q_\infty c}$$

where values of C_μ are obtained by varying the jet total pressure, total temperature, and slot height. The airfoil drag coefficient is modified to account for the added effect of jet thrust. With this modification, it is possible to obtain negative values of C_d at high jet blowing rates.

Turbulence Model

Accurate turbulence models are required to simulate the curved shear-layer flow and to determine the point of boundary-layer separation from the Coanda surface on a circulation control airfoil. In this study, the algebraic turbulence model of Baldwin-Lomax¹⁰ is used with modifications following Bradshaw¹¹ to account for the curved flow over the Coanda surface. The Baldwin-Lomax turbulence model uses the following relation for the eddy viscosity

$$(\mu_t)_{\text{inner}} = \rho |\omega| l^2$$

Bradshaw empirically adjusts the magnitude of the mixing length l to account for streamline curvature by multiplying it by a curvature correction factor

$$F = 1 - \theta S$$

where

$$S = (U/r)/(\partial U/\partial n)$$

All of the quantities necessary to determine the curvature correction factor can be found from the flowfield solution with the exception of θ , which is the empirical curvature correction constant.

The mixing-length correction is in proper agreement with the experimentally observed physics of curved shear-layer flows over convex surfaces.¹¹ Its influence on the Baldwin-Lomax turbulence model is illustrated in Fig. 2 using a typical boundary-layer profile downstream of the slot exit over a Coanda surface. Note that the convex curvature of the Coanda surface has one of two effects on the boundary layer depending on the gradient of local velocity in the direction normal to the surface, $\partial U/\partial n$. The boundary layer tends to become more stable in regions where $\partial U/\partial n$ is positive and more unstable in regions where $\partial U/\partial n$ is negative. The empirical curvature constant θ effectively determines the magnitude of the mixing-length correction in regions of curvature. When $\theta = 0$, no curvature correction is applied and the standard Baldwin-Lomax turbulence model is used. For values of $\theta > 0$, a

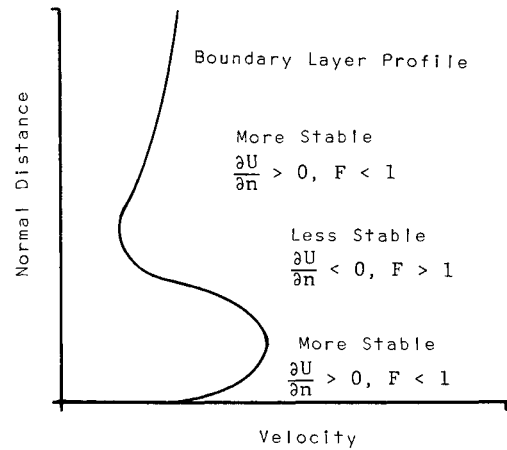


Fig. 2 Wall-jet profile and correction factors downstream of slot.

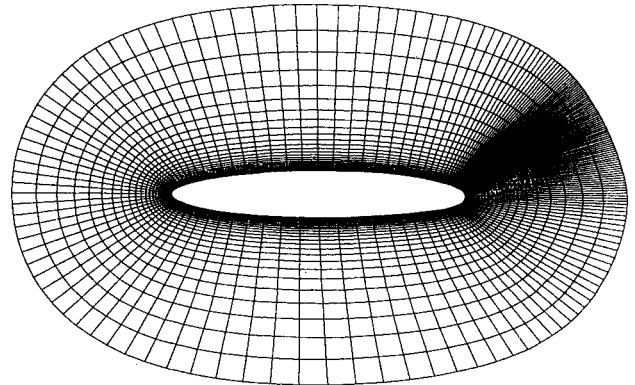


Fig. 3 Interior region of grid.

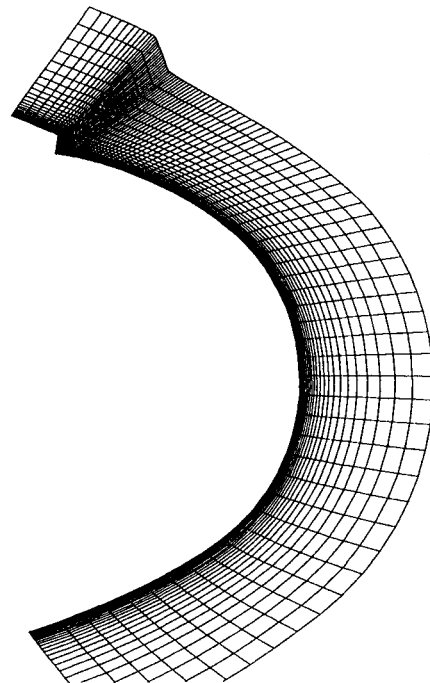


Fig. 4 Jet-slot and Coanda surface region of grid.

proportionally greater curvature correction is applied to the Baldwin-Lomax turbulence model.

Bradshaw¹¹ cautions that this model should only be used as a linear correction. From the limited experimental data available, he suggests that $0.5 < F < 1.5$. These bounds limit the influence of the curvature correction to the linear range and alleviate some of the difficulties encountered when the correction encounters velocity minima or maxima. A curva-

ture correction constant with a value $\theta = 6$ is suggested for unstable wall jets.¹¹

The boundary-layer transition criteria used in this study are different than those proposed by Baldwin-Lomax¹⁰ and are based on discussion provided by Schlichting¹⁸ that includes the effects of Reynolds number and pressure gradient on transition location. The transition location downstream of the forward stagnation point on both upper and lower airfoil surfaces is first determined by assuming that the point of boundary-layer instability is identical to the point of boundary-layer transition. This point can be found given the flight Reynolds number and slenderness ratio of an elliptical shape using potential theory and the Pohlhausen method.¹⁸ The effect of pressure gradient is then modeled by determining if a pressure minimum exists between the forward stagnation point and the computed transition location based on Reynolds number. If such a pressure minimum exists, transition is assumed to occur at the upstream point of minimum pressure.

Drag results using this transition criteria will tend to be somewhat higher than would be expected experimentally. It is well known that the magnitude and sign of the pressure gradient can also be important in determining transition location. In addition, the point of boundary-layer instability usually is a short distance upstream of the transition location.¹⁸ These factors have been ignored in this analysis. As a result, the computed boundary layers over the airfoil surface may be more turbulent than found experimentally, resulting in increased drag.

Grid

The grid topology used in this study is a conventional O-grid, with the grid cutline extending from the airfoil nose to the outer boundary. An algebraic grid was first constructed to obtain the desired point distribution and then refined using an elliptic smoother to obtain a more orthogonal grid. The characteristics of the grid used in this study were based on a sensitivity study of the effect of grid resolution on the computational solution balanced with the requirement of reasonable computer run times.

The outer boundary of the grid used in this study is circular and is located 14 airfoil chords from the airfoil surface. The size of the grid is 176 points in the wraparound direction with 80 points in the normal direction. These points are clustered in areas of the grid where large flowfield gradients exist such as the boundary layer, near the airfoil nose, the jet slot, and over the Coanda surface. A portion of the grid displaying the airfoil and the grid point spacing is shown in Fig. 3, and an enlargement of the jet-slot region is shown in Fig. 4.

One difficulty in using the O-grid topology on circulation control airfoil geometries is due to sharp corners in the airfoil contour at the slot exit where there is a high degree of grid skewness. The effect caused by the lack of grid orthogonality and the resulting poor transformation metrics in the slot region on the computational results is unknown.

Two different types of computers were used to solve the Navier-Stokes equations used in this study. Most results were obtained on a Floating Point Systems M64-20 Minisupercomputer. This 64-bit precision computer has 32 megabytes (MB) of memory and performs at a speed of 6 million floating point

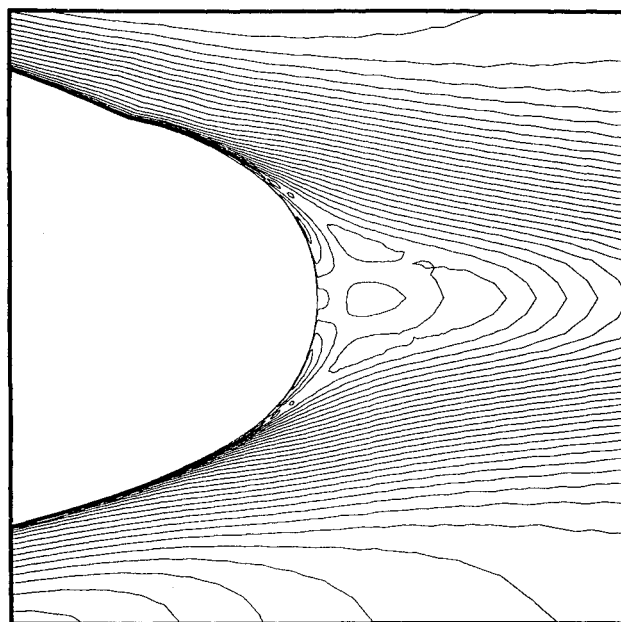


Fig. 5 Coanda surface region Mach contours: $C_\mu = 0$; $\theta = 6$.

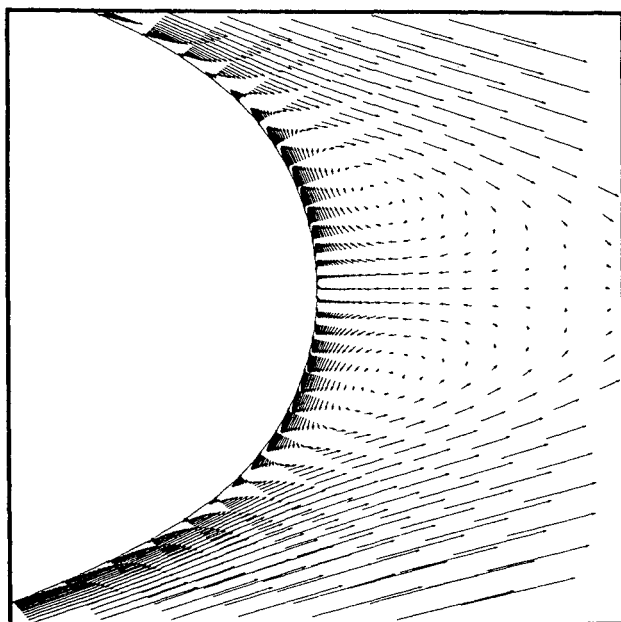


Fig. 6 Coanda surface region velocity vectors: $C_\mu = 0$; $\theta = 6$.

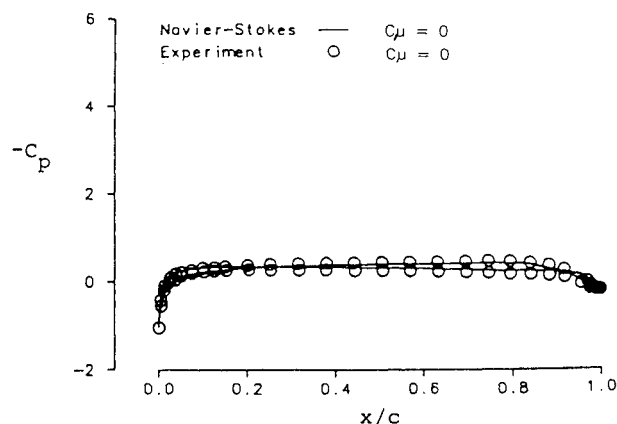


Fig. 7 Pressure coefficient distributions.

Table 1 103RE airfoil experimental and computational test conditions

| $M_\infty = 0.3$, $Re \approx 3.1 \times 10^6$, $\alpha = 0$ deg, $h = 0.0023c$, $\theta = 6$ | | | | | | |
|--|------------------|----------------|----------------|----------------------|----------------|----------------|
| $(C_\mu)_{wt}^a$ | $(C_\mu)_{NS}^a$ | $(C_l)_{wt}^a$ | $(C_l)_{NS}^a$ | α_{eff} , deg | P_l/P_∞ | T_l/T_∞ |
| 0.0000 | 0.0000 | 0.17 | 0.03 | -0.25 | 1.00 | 1.00 |
| 0.0094 | 0.0096 | 0.62 | 0.53 | -0.92 | 1.14 | 0.96 |
| 0.0179 | 0.0187 | 1.11 | 1.00 | -1.66 | 1.28 | 0.93 |
| 0.0322 | 0.0332 | 1.76 | 1.62 | -2.65 | 1.57 | 0.91 |

^aThese results are also plotted in Fig. 12.

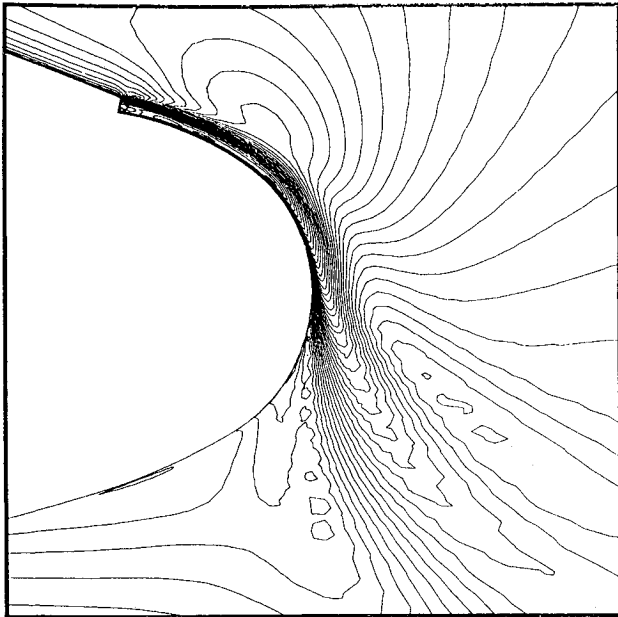


Fig. 8 Coanda surface region Mach contours: $C_\mu = 0.0332$; $\theta = 6$.

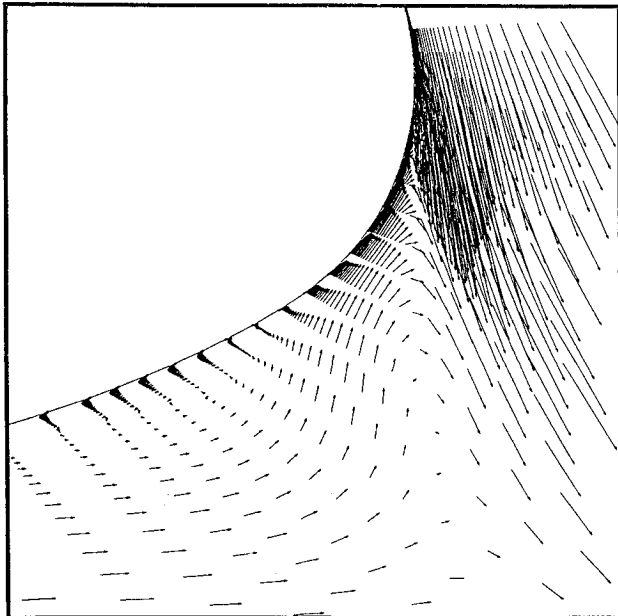


Fig. 9 Coanda surface region velocity vectors: $C_\mu = 0.0332$; $\theta = 6$.

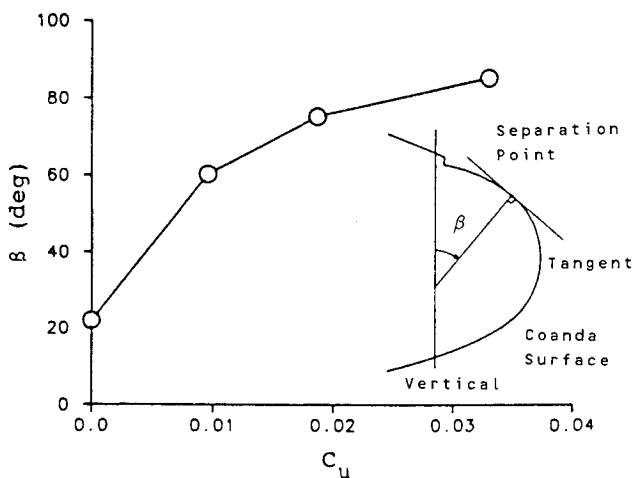


Fig. 10 Effect of momentum coefficient on jet separation point: $\theta = 6$.

operations per second (MFLOPS). This machine is capable of parallel processing and able to take advantage of the vectorizable FORTRAN code of the Navier-Stokes method. A Digital Equipment Corporation VAXstation III/GPX Workstation was also used to obtain solutions in this study. This 32-bit precision computer has 8 MB of memory and an execution speed of approximately 2 MFLOPS.

Airfoil Geometry

The airfoil chosen for analysis in this study is the 103RE airfoil that was designed at the David Taylor Naval Ship Research and Development Center for application as a circulation control helicopter rotor.¹⁹ One of the reasons this airfoil was chosen is due to the extensive wind-tunnel test data available. The airfoil contour is a modified ellipse with a maximum camber of 1% chord located at 70% chord with a reduced leading-edge radius. The airfoil maximum thickness is 16% chord. The jet nozzle is a converging nozzle with the exit (jet slot) located at 96.88% chord. The blunt trailing-edge surface is a reduced ellipse with the radius of curvature varying from 4.6% chord at the slot to 2.8% chord at the airfoil trailing edge. The jet-slot height is 0.0020c.

Results and Discussion

Solutions were obtained by applying the computational Navier-Stokes method to simulate the experimental wind-tunnel test conditions and $(C_\mu)_{wt}$ values shown in Table 1. For example, $(C_\mu)_{NS}$ values used in the simulations were within 5% of those identified in the experiments. The runs in the wind tunnel were performed at a geometric angle of attack of 0 deg; however, the following correction was applied to the simulations to account for tunnel wall interference²⁰:

$$\alpha_{eff} = \alpha - 1.5(C_l)_{wt}$$

The experimental values of lift and pitching moment were obtained by integrating the airfoil pressure distributions, and the drag values were obtained by using a wake probe.¹⁹ A jet-slot height of 0.0023c was used for the simulations since it was established in the experiments that when the jet plenum was pressurized the slot heights increased from 0.0020c to as much as 0.0023c.¹⁹

For the no-blowing case where $C_\mu = 0$, the computed Mach contour solution in the vicinity of the trailing edge is shown in Fig. 5 and the corresponding velocity vectors are shown in Fig. 6. The flow separation locations in the blunt trailing-edge region are clearly visible in Figs. 5 and 6, and the relatively symmetrical counter-rotating vortices can be seen in Fig. 6. The pressure distributions about the airfoil obtained in the simulation agreed closely with those reported in the experiment, as shown in Fig. 7. The slight effect of airfoil camber on the pressure distribution is apparent on the upper surface over the aft portion of the airfoil.

Mach contours and velocity vectors in the trailing-edge region are shown in Figs. 8 and 9 for $C_\mu = 0.0332$. With blowing, the flow about the airfoil changed considerably, as shown visibly by the Mach contours and velocity vectors. As blowing increased, the forward and aft stagnation points and the trailing-edge vortices and separation points moved farther around toward the lower surface. Figures 8 and 9 show the jet and how the stagnation and separation points and vortex regions have moved to the lower surface. The separation point on the upper surface of the trailing edge, as measured by the angle β , is shown as a function of C_μ in Fig. 10. At the highest C_μ , the flow has been turned almost 90 deg, as illustrated in Figs. 8 and 9.

The pressure distributions around the airfoil for $C_\mu = 0.0332$ are shown in Fig. 11. The agreement between the simulation and the experiment is reasonably good, except at the leading and trailing edges where the computational results underpredict the amount of suction.

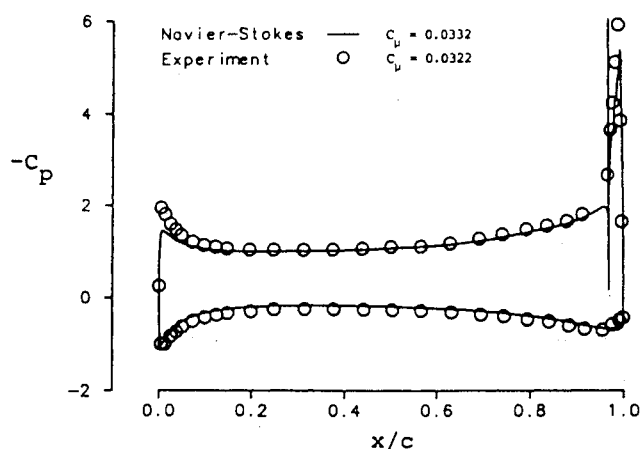


Fig. 11 Pressure coefficient distributions.

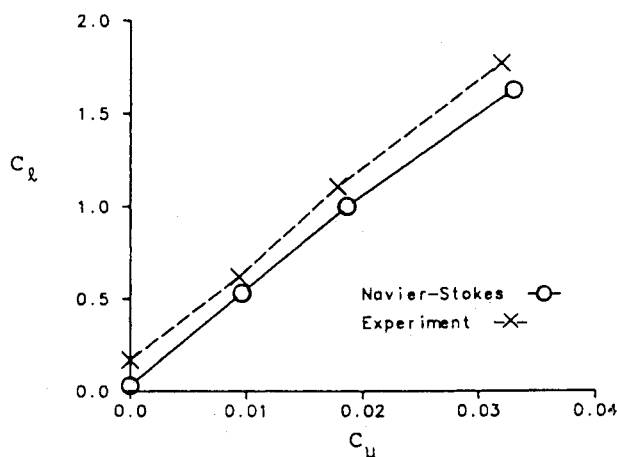


Fig. 12 Effect of jet blowing on computed and experimental lift coefficients.

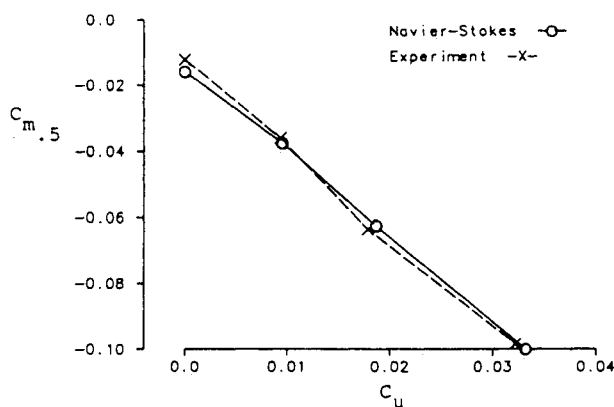


Fig. 13 Effect of jet blowing on computed and experimental moment coefficients.

Computed and experimental values of the lift, moment, and drag coefficients are plotted as a function of C_μ in Figs. 12, 13, and 14, respectively. These results were obtained for a value of $\theta = 6$. The experimental and computational values of C_l are in close agreement and vary approximately linearly with C_μ . Differences between experimental and computed values of C_l may be caused by the turbulence model with $\theta = 6$, and, as will be shown later, adjustments to θ reduced the differences and improved agreement. With $\theta = 6$, premature separation of the jet boundary layer at the trailing edge may have occurred, which would decrease the lift. This is possible since θ controls the degree of turbulent transport within the boundary layer over the curved surface.

The pitching moment results are shown in Fig. 13, and the agreement between the experiment and the computation is good. As C_μ increases, the nose-down pitching moment increases, as expected. The high suction pressures on the Coanda surface, coupled with a long moment arm, generate a large nose-down pitching moment.

The variation of drag coefficient with blowing momentum coefficient is shown in Fig. 14. Although the computational and experimental results offer similar trends, the agreement is not as good as with the other aerodynamic coefficients. The cause for this lack of agreement is not known, but the turbulence model transition criteria, as discussed earlier, and the upstream insertion of momentum from the jet slot may be contributing factors. Other factors could be differences in the calculation of the drag coefficient and the inaccuracies of measuring airfoil drag in the wind tunnel with a wake probe.

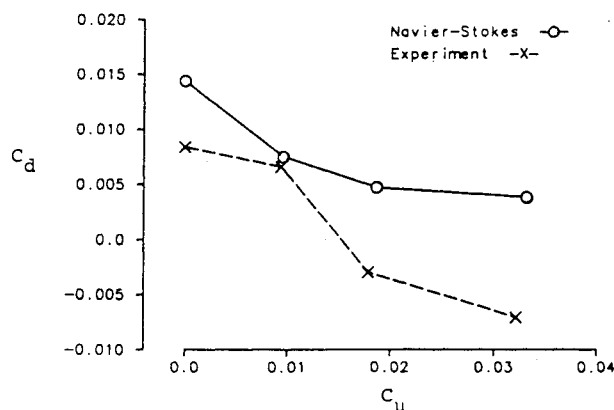
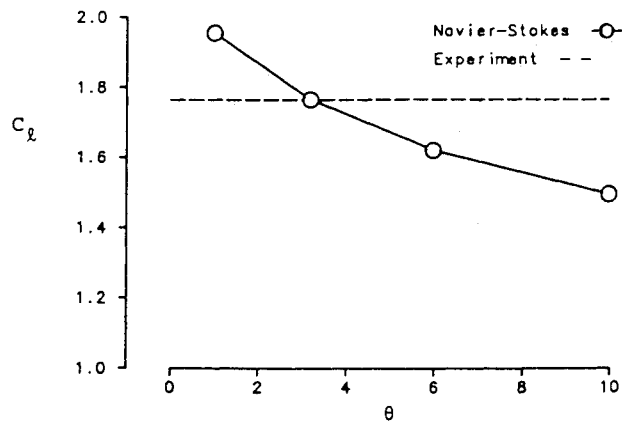
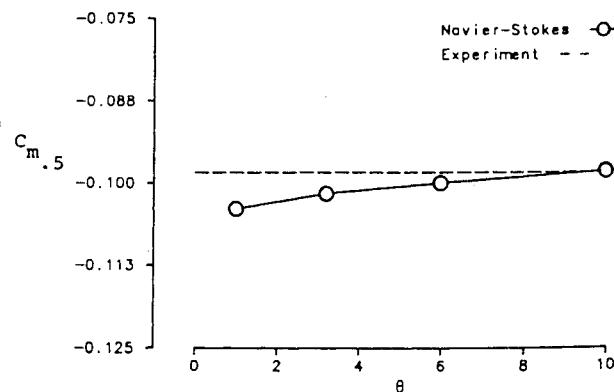


Fig. 14 Effect of jet blowing on computed and experimental drag coefficients.

Fig. 15 Effect of curvature constant on lift coefficient: $C_\mu = 0.0332$.Fig. 16 Effect of curvature constant on moment coefficient: $C_\mu = 0.0332$.

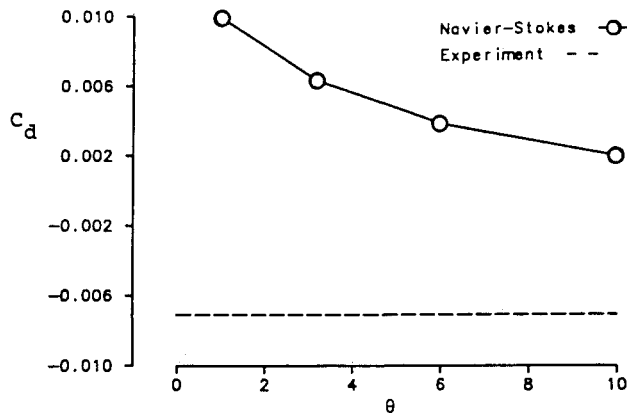


Fig. 17 Effect of curvature constant on drag coefficient: $C_\mu = 0.0332$.

The empirical curvature constant θ was varied from 1 to 10 to determine the effect of θ on the computations and to see if better agreement with experiment could be obtained. The effects of θ on C_l , $C_{m,5}$, and C_d are shown in Figs. 15, 16, and 17, respectively. The results show that C_l and C_d are quite sensitive to values of θ , whereas $C_{m,5}$ is not as sensitive. For C_l , the best agreement with experiment was obtained for $\theta = 3.2$, but the best agreement with experiment for $C_{m,5}$ and C_d occurred at larger values of θ . Also, a replot of Fig. 11 showed that the computed C_p with $\theta = 3.2$ agreed more closely with experiment at the leading and trailing edges than with $\theta = 6$. These results indicate that further work is needed for the modeling of the flow about the Coanda surface. This is in agreement with the conclusion of others.^{3,5,6}

Conclusions

A computational procedure was developed and numerical solutions were obtained that predict the aerodynamic coefficients of a circulation control airfoil. The results were shown to depend on an empirical curvature constant in the turbulence model to account for the curved flow over the blunt trailing edge. Although the results are promising, it is evident that additional work is needed to develop accurate turbulence models for circulation control airfoils.

References

- ¹Kohlman, D. L., *Introduction to V/STOL Airplanes*, Iowa State University Press, Ames, IA, 1981.
- ²Englar, R. J., Trobaugh, L. A., and Hemmerly, R. A., "STOL Potential of the Circulation Control Wing for High Performance Aircraft," *Journal of Aircraft*, Vol. 15, No. 3, 1978, pp. 175-181.
- ³Wood, N., and Nielsen, J., "Circulation Control Airfoils Past, Present, Future," AIAA Paper 85-0204, AIAA 23rd Aerospace Sciences Meeting, Reno, NV, Jan. 1985.
- ⁴Nielsen, J. N., and Biggers, J. C., "Recent Progress in Circulation Control Aerodynamics," AIAA Paper 87-0001, AIAA 25th Aerospace Sciences Meeting, Reno, NV, Jan. 1987.
- ⁵Pulliam, T. H., Jespersen, D. C., and Barth, T. J., "Navier-Stokes Computations for Circulation Control Airfoils," *Proceedings of the Circulation Control Workshop 1986*, NASA CP-2432, May 1987, pp. 135-164.
- ⁶Shrewsbury, G. D., "Numerical Study of a Research Circulation Control Airfoil Using Navier-Stokes Methods," *Journal of Aircraft*, Vol. 26, No. 1, 1989, pp. 29-34.
- ⁷Shrewsbury, G. D., "Analysis of Circulation Control Airfoils Using an Implicit Navier-Stokes Solver," AIAA Paper 85-0171, AIAA 23rd Aerospace Sciences Meeting, Reno, NV, Jan. 1985.
- ⁸Shrewsbury, G. D., "Numerical Evaluation of Circulation Control Airfoil Performance Using Navier-Stokes Methods," AIAA Paper 86-0286, AIAA 24th Aerospace Sciences Meeting, Reno, NV, Jan. 1986.
- ⁹Berman, H. A., "A Navier-Stokes Investigation of a Circulation Control Airfoil," AIAA Paper 85-0300, AIAA 23rd Aerospace Sciences Meeting, Reno, NV, Jan. 1985.
- ¹⁰Baldwin, B. S., and Lomax, H., "Thin Layer Approximation and Algebraic Model for Separated Turbulent Flows," AIAA Paper 78-257, AIAA 16th Aerospace Sciences Meeting, Huntsville, AL, Jan. 1978.
- ¹¹Bradshaw, P., "Effects of Streamline Curvature on Turbulent Flow," North Atlantic Treaty Organization, Technical Editing and Reproduction Ltd., London, AGARDograph No. 169, Aug. 1973.
- ¹²Beam, R. M., and Warming, R. F., "An Implicit Factored Scheme for the Compressible Navier-Stokes Equations," *AIAA Journal*, Vol. 16, No. 4, 1978, pp. 393-402.
- ¹³Visbal, M. R., "Calculation of Viscous Transonic Flows About a Supercritical Airfoil," Air Force Wright Aeronautical Labs., Wright-Patterson AFB, OH, TR-86-3013, July 1986.
- ¹⁴Visbal, M. R., "Evaluation of an Implicit Navier-Stokes Solver for Some Unsteady Separated Flows," AIAA Paper 86-1053, AIAA/ASME 4th Fluid Mechanics, Plasma Dynamics, and Lasers Conference, Atlanta, GA, May 1986.
- ¹⁵Visbal, M. R., and Shang, J. S., "Numerical Investigation of the Flow Structure around a Rapidly Pitching Airfoil," AIAA Paper 87-1424, AIAA 19th Fluid Dynamics, Plasma Dynamics, and Lasers Conference, Honolulu, HI, June 1987.
- ¹⁶Steger, J. L., "Implicit Finite-Difference Simulations of Flow About Arbitrary Two-Dimensional Geometries," *AIAA Journal*, Vol. 16, No. 7, 1978, pp. 679-686.
- ¹⁷Williams, S. L., "Use of Navier-Stokes Methods to Predict Circulation Control Airfoil Performance," M. S. Thesis, Air Force Institute of Technology, Wright-Patterson AFB, OH, AFIT/GAE/AA/89M-4, March 1989.
- ¹⁸Schlichting, H., *Boundary-Layer Theory*, 7th ed., McGraw-Hill, New York, 1979.
- ¹⁹Abramson, J., and Rogers, E. O., "High-Speed Characteristics of Circulation Control Airfoils," AIAA Paper 83-0265, AIAA 21st Aerospace Sciences Meeting, Reno, NV, Jan. 1983.
- ²⁰Abramson, J., private communication, David Taylor Naval Ship Research and Development Center, Bethesda, MD, Nov. 1988.